

# Measurements of resistivity of nitrogen-doped single crystals of type Ib diamond by the van der Pauw method with Ti–Pt contacts in the temperature range 573–1000 K

© S.G. Buga<sup>1</sup>, G.M. Kvashnin<sup>1</sup>, M.S. Kuznetsov<sup>1</sup>, N.V. Kornilov<sup>1</sup>, N.V. Luparev<sup>1</sup>, M. Yao<sup>2</sup>

<sup>1</sup> Technological Institute for Superhard and Novel Carbon Materials, 108840 Moscow, Troitsk, Russia

<sup>2</sup> State Key Laboratory of Superhard Materials, Jilin University, 130012 Changchun, China

E-mail: buga@tisnum.ru

Received April 20, 2023

Revised June 2, 2023

Accepted June 26, 2023

The electrical resistivity values of square diamond plates doped with nitrogen in the form of *C*-centers with concentrations of 5; 55; 140 ppm are measured by the van der Pauw method in the temperature range of 573–1000 K. Based on the results of the analysis of the primary measurement data, the resistivity values are calculated in the approximation of point ohmic Ti–Pt contacts, as well as taking into account the actual dimensions of triangular angular contacts. It was found that up to the temperature limit of  $930 \pm 50$  K the differences in the resistivity values obtained by three different methods of the experimental data analysis do not exceed 3–7%. Ti–Pt contacts may be used in microelectronic and quantum optoelectronic devices based on nitrogen-doped diamonds.

**Keywords:** *n*-type semiconductor diamond, nitrogen doping, ohmic contacts, resistivity.

## 1. Introduction

Semiconductor diamond single-crystals and multilayer structures based on them are finding ever wider areas of application in electronics, quantum optoelectronics, and sensors [1–13]. For example, boron-doped diamonds are used in power and high-frequency Schottky diodes [1–4], as well as in converters of  $\beta$ -radiation energy of radioactive isotopes into electrical power [5]. Bipolar diamond semiconductor devices most often use layers with hole type conductivity bulk-doped with boron and layers with electronic conductivity doped with phosphorus [6]. Currently, phosphorus is the main donor-type dopant, because the activation energy of phosphorus atoms in the diamond lattice is lower than that of other donor atoms and varies in the range of 0.3–0.5 eV depending on the concentration and degree of compensation [14]. Another main donor-type dopant in diamond is nitrogen in the form of single substitution atoms (*C*-centers), however, their activation energy is much higher, 1.7 eV [15,16], which significantly limits the use of such diamonds in active electronics. Nevertheless, diamond single-crystals doped with nitrogen in the form of *C*-centers (type Ib according to the commonly used classification of diamonds [17,18]) are widely used as substrates for the manufacture of multilayer diamond structures of various types. This is mainly due to the fact that the growth processes of nitrogen-containing diamond single-crystals are well established and their cost is significantly lower compared to high-purity undoped diamonds. At the same time, despite the high activation energy of nitrogen donors, type Ib diamonds are already effectively used not only as passive structural elements, but also as active

layers of unipolar and bipolar devices operating at room temperature [7,8]. Due to their high thermal, chemical, radiation resistance and mechanical strength, semiconductor diamonds are promising materials for high-temperature and extreme electronics. In this regard, studies of electrical and optoelectronic properties of various doped synthetic diamond single-crystals in a wide temperature range from cryogenic to 800–900 K and more remain relevant. In addition, metal contacts are necessary for quantum optoelectronic devices and sensors based on nitrogen-vacancy centers, such as single-photon light sources, quantum computers and telecommunication devices [9,10], ultra-sensitive magnetometers, spin gyroscopes, etc. [11–13]. The application of nanoscale metal contacts to such devices based on nitrogen-doped diamonds is important for the development of their functional parameters. In this regard, the production of metal contacts for type Ib diamonds and the study of their characteristics remains a relevant problem.

For hole-type diamonds, the technology for manufacturing ohmic metal contacts with low contact resistance has already been well developed. For this purpose, two- or three-layer metallization is mainly used based on carbide-forming metals, primarily titanium, with intermediate high-temperature carbidization, and subsequent deposition of platinum and gold layers [19–22]. Contacts made in the same way for donor-doped diamonds are also ohmic to a fairly high degree, but there is still not enough information about the value of contact resistance and its dependence on the degree of doping of these diamonds. Thus, the task of studying the electrical properties of *n*-type diamond single-crystals in a wide temperature range up to 1000 K

and more, and manufacturing stable ohmic and rectifying metal contacts for them remains relevant so far.

A standard and convenient method for measuring resistivity and Hall coefficient of semiconductor materials is the four-point probe method of van der Pauw [23]. For precision measurements, this method requires the manufacture of low-resistance contacts. However, due to the low electronic work function in *n*-type diamonds, the manufacture of such contacts, stable in the temperature range up to 1000 K, remains a difficult task.

This study is devoted to the analysis of the effect of corner Ti–Pt contacts of finite dimensions, fabricated on the surface of thin square wafers of type Ib synthetic diamond single-crystals with different nitrogen concentrations, on the results of resistivity measurements by the van der Pauw method in the temperature range of 573–1000 K.

## 2. Experimental samples and measurement procedures

The studies were carried out on three samples cut from synthetic Ib single-crystals with different concentrations of nitrogen *C*-centers. Two initial single-crystals were grown by the method of temperature gradient at high pressure (TG-HPHT) [24,25]. One more crystal was grown by the method of homoepitaxial chemical vapor deposition (CVD method) [2,26] on a substrate in the form of a wafer cut from a single-crystal produced by the TG-HPHT method. After the CVD-growth, the substrate was separated from the grown layer with a thickness of 0.25 mm using laser cutting. All three samples in the form of thin square wafers with crystallographic orientation (100) were cut from the original crystals using laser cutting and then mechanically polished. Possible surface contamination caused by mechanical polishing was removed by etching in boiling „aqua regia“ for 2 hours, followed by washing in deionized water and annealing in the atmosphere at  $T = 680^\circ\text{C}$  for 20 min.

The concentration of *C*-centers in wafers made from single-crystals grown by the HPHT method was determined by IR spectroscopy, and in a wafer made by the CVD method the concentration was determined by absorption in the visible range [17]. Dimensions of the samples, concentration of *C*-centers, and relative total area of metal contacts are given in the table.

After spectroscopic studies, corner Ti contacts with a thickness of 5 nm were deposited on one of the large surfaces of the wafer with an area of  $S$  through contact masks using magnetron sputtering. After this, to obtain a titanium carbide sublayer, annealing was carried out at  $T = 650^\circ\text{C}$  for 20 min. Then, a layer of Pt with a thickness of 200 nm was deposited, which prevents the oxidation of titanium in the air and has a good adhesion under subsequent heating in the process of measurements in the range of up to 1000 K. Electrical leads in the form of gold wires with a diameter of  $40\ \mu\text{m}$  were welded to the

Dimensions of the experimental samples, concentrations of *C*-centers, and relative total area of metal contacts  $A$ , %

Sample No.	Dimensions, mm <sup>3</sup>	A, %	$N_C$ , ppm
1	$4.0 \times 4.0 \times 0.43$	22	140
2	$2.6 \times 2.6 \times 0.25$	9	55
CVD	$2.5 \times 2.5 \times 0.25$	12	5

fabricated contact pads using thermocompression welding. Photos of fabricated samples with contact pads and welded microwires are shown in Figure 1. To assess the degree of influence of the total contact area  $S_c$  on the accuracy of determining the real resistivity  $\rho$  of the samples, the coefficients of the relative contact area  $A = S_c/S$  given in the table in % were used.

Electrical measurements were carried out by the van der Pauw four-point probe method using a LakeShore™ Cryotronics 7707A HMS system. The samples were heated in an argon atmosphere in a sealed Linkam-1000TS heater, providing a maximum temperature of  $1000^\circ\text{C}$ .

The resistivity  $\rho$  of the samples was calculated on the basis of the primary experimental data by the van der Pauw method in three ways. In the first method, to calculate  $\rho_1$ , the inherent software algorithm of the LakeShore™ Cryotronics 7707A HMS system was used, which involves measurement of samples with „point“ corner ohmic contacts, i.e. contacts with a total area  $S_c$  significantly smaller than that of the sample, i.e.  $A \ll 1$ . In fact, in our experiment this condition was generally not met, which knowingly led to an additional systematic error in determining the resistivity of the samples.

The calculation of  $\rho_2$  by the second method was carried out using the refined formula of the van der Pauw method [23] using the complete set of experimental data obtained  $R_{ij,kl}$ :

$$\rho_2^{ij,kl} = \frac{\pi d}{\ln 2} \frac{R_{ij,kl} + R_{jk,li}}{2} \left[ 1 - \frac{\ln 2}{2} \left( \frac{R_{ij,kl} - R_{jk,li}}{R_{ij,kl} + R_{jk,li}} \right)^2 \right], \quad (1)$$

where  $d$  is thickness of the diamond wafer. The indices  $ij$  and  $kl$  cyclically took on the values of 1, 2, 3, 4.  $\rho_2$  was averaged over all four pairs of contacts.

To determine  $\rho_3$  in the third way, the results of modeling the distributions of current lines and equipotential surfaces in the samples under study using the COMSOL Multiphysics™ software package were used. The modeling took into account the real geometric dimensions of all contact pads and their relative position on each of the samples.

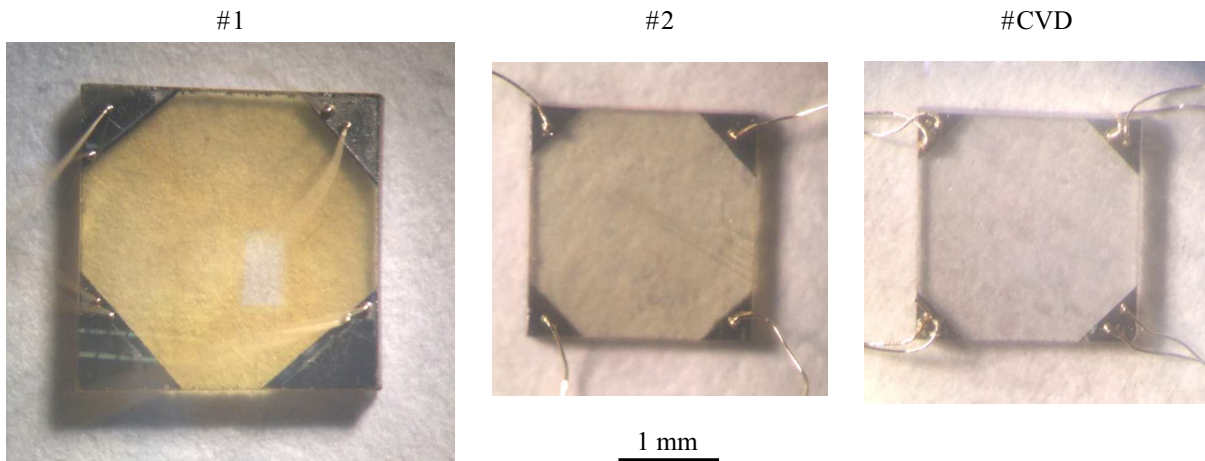


**Figure 1.** Samples of square wafers cut from nitrogen-doped diamond single-crystals with corner contacts of various sizes and welded gold microwires for electrical resistance measurements using the van der Pauw method.

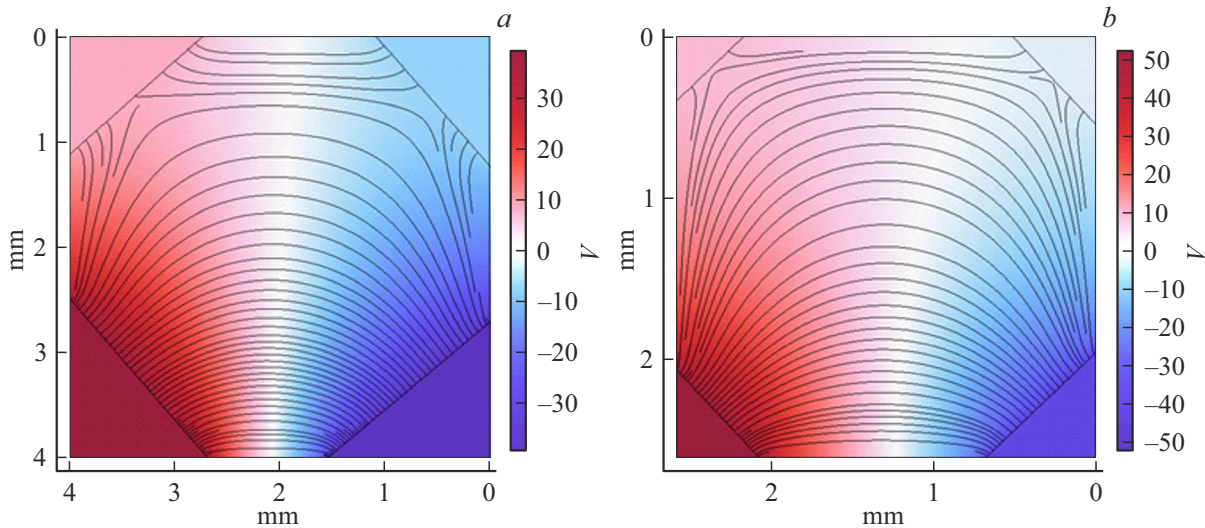


**Figure 2.** Models of the distribution of electric potential  $V$  and density of current lines  $J$  on the surface of samples 1 (a) and 2 (b) at  $T = 700$  K. (The colored version of the figure is available on-line).

To calculate the resistivity we used the linear relationship

$$R_{ij,kl} = \frac{U_{ij}}{I_{kl}} = \rho_2 F_{ij,kl}, \tag{2}$$

where  $U_{ij}$  is induced potential difference between contacts  $i$  and  $j$ ,  $I_{kl}$  is current given by an external source through contacts  $k$  and  $l$ ,  $F_{ij,kl}$  is form factor depending on size, shape, and location of sample contacts,  $ij$  and  $kl$  are indices cyclically changing from 1 to 4. Initially, when modeling a specific sample, a certain test value of resistivity was specified, determined by the 1-st method, for example,  $\rho_0$ . Then,  $R_{ij,kl}^0$  values corresponding to it were determined. Then, the form factor of the sample was calculated using the following formula:

$$F_{ij,kl} = \frac{R_{ij,kl}^0}{\rho_0}. \tag{3}$$

Then, the experimental resistivity of the diamond wafer was calculated as:

$$\rho_{ij,kl}^{\text{exp}} = \frac{R_{ij,kl}^{\text{exp}}}{F_{ij,kl}} \tag{4}$$

for each quadruple of contacts ( $ij, kl$ ). The final value of  $\rho_3$  was determined as the average of four  $\rho_{ij,kl}^{\text{exp}}$  values.

Thus, in the third method, when calculating  $\rho_3$ , fulfilment of the  $A \ll 1$  condition is not required. As a result of the simulation, distribution diagrams of electric potential  $V$  and density of electric current lines  $J$  on the surface of all studied samples were obtained in the temperature range of 573–1000 K. Figure 2 shows examples of such distributions for samples 1 (a) and 2 (b) at  $T = 700$  K. Similar distributions in the sample bodies differ insignificantly from the distributions on the surface.

The red and blue colors in Figure 2 indicate areas of positive and negative potential, respectively. Color intensity displays the potential value in volts according to the right vertical color scale. The white extended areas in Figure 2 are areas of zero potential. For sample 2, this line is noticeably shifted towards the electrodes on the right, the area of which is noticeably larger than the area of the contacts on the left. Such a noticeable inhomogeneity of the potential distribution in the sample results in a significant difference in the measured induced potentials at adjacent pairs of contacts. In addition to non-point form of the contacts, this also leads to an additional error caused by their unequal sizes.

### 3. Experimental results and analysis thereof

Figure 3 shows temperature dependences of resistivity of the studied samples, determined by the van der Pauw method using procedures 1 and 3 described above.

As can be seen in Figure 3, for all three measured samples the resistivities determined by procedures 1 and 3 are very close to each other. To clarify in more detail the influence of contact sizes and calculation methods on the resistivity, temperature dependences of the ratios  $\rho_2/\rho_1$ ,  $\rho_3/\rho_1$ , and  $\rho_3/\rho_2$  were plotted (Figure 4). The discrepancies between the obtained dependences reflect the influence of the calculation methods used in this study on the value of the sample resistivity being determined.

As can be seen from the graphs in Figure 4, in all three samples the resistivity  $\rho_2$  calculated by formula (1) using the full set of experimental data is slightly higher than the  $\rho_1$  values determined using the built-in algorithm of the experimental setup. The largest deviation is observed at the edges of the measurement ranges, especially at  $T < 600$  K for sample 2, which may be due to the very high resistance of the sample below this temperature and the large measurement error due to current leaks in the supply cables. At  $T > 830$  K in the CVD sample and at  $T > 900$  K in sample 1, also an increase in the ratio  $\rho_2/\rho_1$  to  $\sim 1.08$  is observed. After completion of the experiments, partial peeling of the metallization of contacts was found, which deteriorates their properties. Depending on the individual features of the samples, this process begins at temperatures of 850–930 K. The main cause for the peeling is the difference in the thermal expansion coefficients of diamond and platinum. As a rule, at temperatures of  $> 1030$  K, complete destruction of contacts takes place. Between the specified low (600–650 K) and high (850–930 K) temperature boundaries for all three samples the  $\rho_2$  is greater than the  $\rho_1$  by 1–5%. The minimum observed difference  $\sim 1\%$  can be considered a systematic measurement error of the device itself when processing the original experimental data, because in these methods of finding resistivity by the van der Pauw method the same assumptions are made regarding the shape of the measured samples and contacts

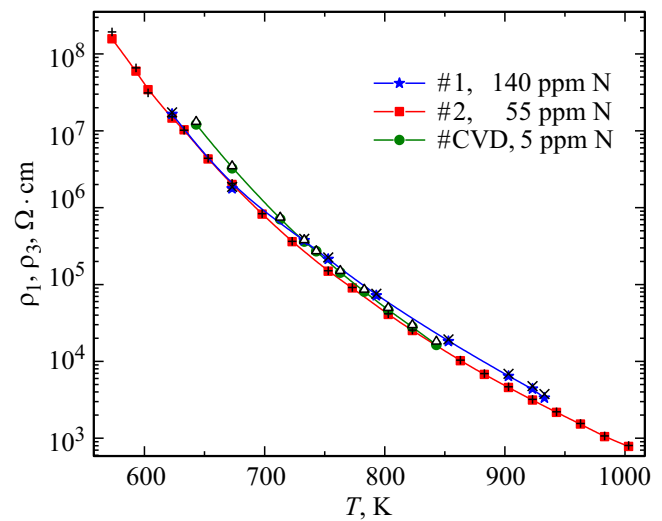


**Figure 3.** Temperature dependences of resistivities  $\rho_1$  (color markers), recorded by the LakeShore™ Cryotronics 7707A HMS system in the approximation of „ideal point contacts“, and  $\rho_3$  (black markers), calculated by modeling in COMSOL Multiphysics™ software taking into account the actual dimensions of the samples and contacts.

to them. Higher deviation values should be considered as individual characteristics of each specific sample.

The largest discrepancy of up to 7% outside the measurement ranges is observed when comparing the experimental values of  $\rho_1$  with the calculated values of  $\rho_3$  obtained by modeling taking into account the actual sizes of contacts to the samples. This is especially noticeable for sample 1 (Figure 2, a). In this case, the  $\rho_3/\rho_2$  ratios are systematically less than  $\rho_3/\rho_1$  for all three samples. The  $\rho_3/\rho_2$  ratios are the closest to 1. The maximum  $\sim 1.05$  ratio in the entire measurement range is observed for sample 1 with the largest contact sizes. For samples 2 and CVD, this ratio is 1.01–1.03, except for a separate point of 1.06 at  $T = 573$  K in sample 2. A measurement error of up to 5% due to the finite dimensions and quality of contacts is acceptable for such measurements.

Ti–Pt contacts have proven themselves to be ohmic and mechanically strong for diamonds with hole type conductivity [19–21], however, in the case of *n*-type diamonds doped with nitrogen there is not enough information yet in support of this statement. In this regard, the investigations carried out in this study make it possible to evaluate the suitability of the manufactured Ti–Pt contacts both in terms of their electrical properties and in terms of thermal stability. Comparison of the results of calculating the resistivity  $\rho_2$  in the approximation of „ideal point contacts“ with  $\rho_3$  obtained by numerical modeling of the distribution of flow currents and induced potentials in the van der Pauw geometry shows good agreement. The difference between  $\rho_2$  and  $\rho_3$  within 2–5% over a wide temperature range can be due to both the actual sizes of the contacts and their contact resistance. The effect of dimensions of contacts located

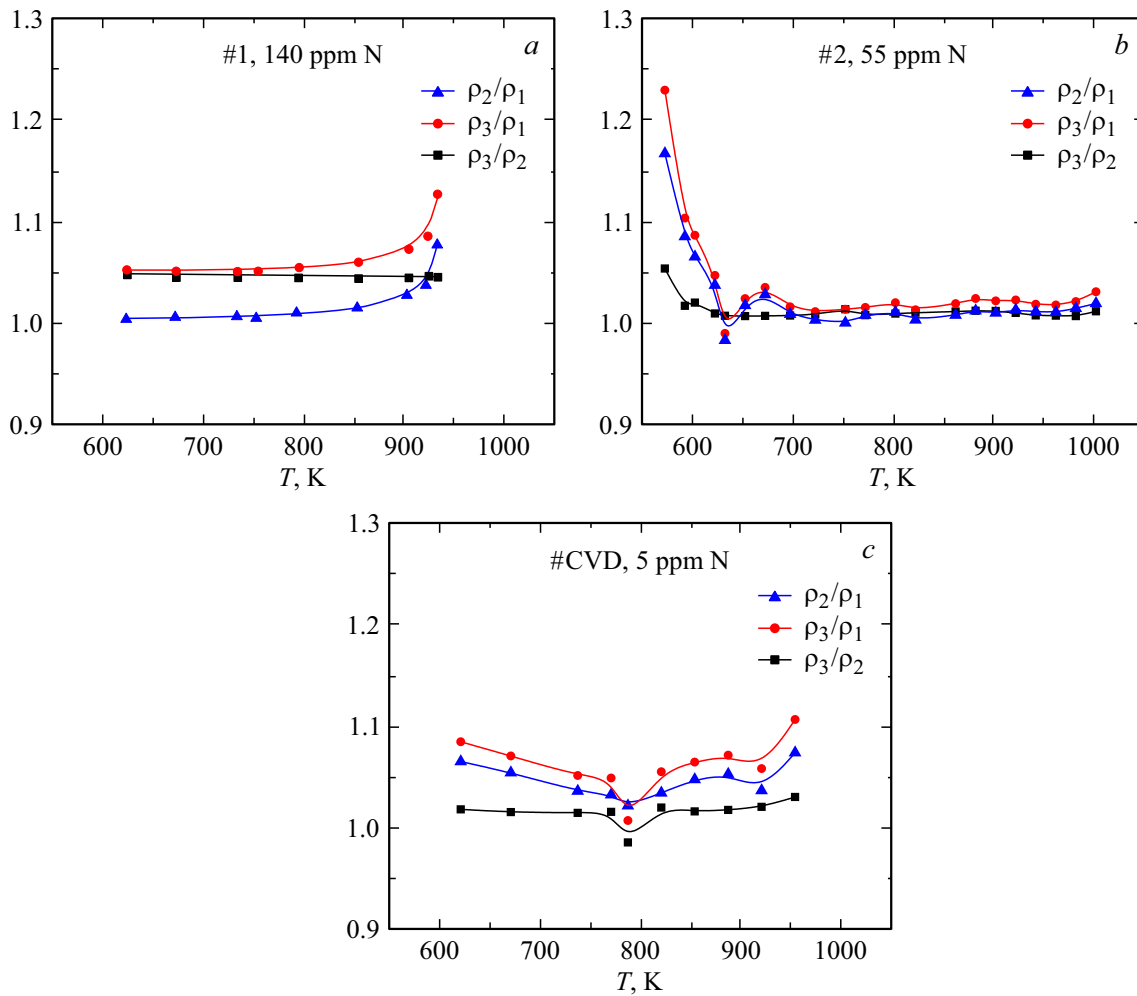


**Figure 4.** Temperature dependences of the ratios of electrical resistivities obtained using the var der Pauw method in three ways for the three studied samples 1 (a), 2 (b), and CVD (c).

on corners of the square sample surface on the resistivity obtained by the var der Pauw method was studied earlier in [27]. It is shown that the correction factor  $k$ , in our case equal to the  $\rho_3/\rho_2$  ratio, for contacts similar to sample 1 should be  $\sim 1.03$ , and for contacts as those on samples 2 and CVD it should be  $\sim 1.015$ . These values are very close to those obtained in our experiments, especially for samples 2 and CVD. The additional deviation of  $\sim 2\%$  for sample 1 may be due to the non-ideal quality of the contacts. In general, the values of 1.03 and 1.05 can be used as correction factors when measuring resistivity by the var der Pauw method for square-shaped samples with triangular corner Ti–Pt contacts similar to those made on samples 2, CVD, and 1, respectively when processing the initial experimental data using the refined formula of the var der Pauw method (1). When using the internal data processing algorithm in the LakeShore™ Cryotronics 7707A HMS system, the correction factor is 1.03–1.07 in the main temperature measurement range but can reach values of 1.1–1.25 at the beginning and end of the range of 573–1000 K. The upper temperature limit for stable

operation of Ti–Pt contacts to nitrogen-doped diamonds is  $900 \pm 50$  K.

## 4. Conclusion

Experimental values of electrical resistivity  $\rho_1$  of three experimental samples of nitrogen-doped single-crystals of type Ib diamonds in the temperature range of 573–1000 K, determined by the var der Pauw method using a software algorithm of the LakeShore™ Cryotronics 7707A HMS system in the approximation of point electrical contacts, on average are 3–7% less than  $\rho_3$  calculated in the COMSOL Multiphysics software package™ taking into account their finite sizes. Also, the  $\rho_1$  values are on average 3–5% less than the calculated resistivities  $\rho_2$  for the case of „ideal“ point contacts, but using a more complete set of experimental data. The values of the correction factor  $k = \rho_3/\rho_2 = 1.02$ –1.05 obtained on the basis of the studies are in good agreement with the values of 1.015–1.03 theoretically calculated earlier [27] for samples of any type.

This confirms the high accuracy of the modeling in nitrogen-doped semiconductor diamonds with *n*-type conductivity in a wide temperature range with concentrations of nitrogen C-centers of 5–140 ppm and, respectively, resistivities from  $8 \cdot 10^3$  to  $2 \cdot 10^8$  Ohm·cm. The difference between the experimental and calculated values of resistivity, that is as high as 20% at  $T < 630$  K, may be indicative of the effect of leakage currents through insulating materials in the connection circuit of samples with an electrical resistance of more than  $\sim 10$  GOhm.

The Ti–Pt contacts are suitable for electrical measurements of nitrogen-doped Ib-diamonds using the van der Pauw method below the temperature of  $900 \pm 50$  K. Also, Ti–Pt contacts can be proposed as current and potential terminals in microelectronic and quantum optoelectronic devices based on Ib type diamonds.

### Funding

This study was supported by grant of the Russian Science Foundation, project No. 22-22-00817, <https://rscf.ru/project/22-22-00817/>.

### Conflict of interest

The authors declare that they have no conflict of interest.

### References

- [1] C.J.H. Wort, R.S. Balmer. *Materials Today*, **11**, 23 (2008).
- [2] S. Koizumi, H. Umezawa, J. Pernot, M. Suzuki. *Power Electronics Device Applications of Diamond Semiconductors. A volume in Woodhead Publishing Series in Electronic and Optical Materials* (Elsevier Ltd, Woodhead Publishing, 2018) p. 433.
- [3] N. Donato, N.C. Rouger, J. Pernot, G. Longobardi, F. Udrea. *J. Phys. D: Appl. Phys.*, **53** (9), 093001 (2019).
- [4] V.S. Bormashov, S.A. Terentiev, S.G. Buga, S.A. Tarelkin, A.P. Volkov, D.V. Teteruk, N.V. Kornilov, M.S. Kuznetsov, V.D. Blank. *Diamond Relat. Mater.*, **75**, 78 (2017).
- [5] V. Bormashov, S. Troschiev, A. Volkov, S. Tarelkin, E. Korostylev, A. Golovanov, M. Kuznetsov, D. Teteruk, N. Kornilov, S. Terentiev, S. Buga, V. Blank. *Phys. Status Solidi A*, **212** (11), 2539 (2015).
- [6] X. Zhang, T. Matsumoto, S. Yamasaki, C.E. Nebel, T. Inokuma, N. Tokuda. *J. Mater. Res.*, **36**, 4688 (2021).
- [7] T. Matsumoto, T. Mukose, T. Makino. *Diamond Relat. Mater.*, **75**, 152 (2017).
- [8] T. Matsumoto, T. Yamakawa, H. Kato, T. Makino, M. Ogura, X. Zhang, T. Inokuma, S. Yamasaki, N. Tokuda. *Appl. Phys. Lett.*, **119**, 242105 (2021).
- [9] S. Pezzagna, D. Rogalla, D. Wildanger, J. Meijer, A. Zaitsev. *New J. Phys.*, **13**, 035024 (2011).
- [10] L. Childress, R. Hanson. *MRS Bulletin*, **38**, 134 (2013).
- [11] L. Rondin, J.-P. Tetienne, T. Hingant, J.-F. Roch, P. Maletinsky, V. Jacques. *Rep. Progr. Phys.*, **77**, 056503 (2014).
- [12] V.V. Soshenko, S.V. Bolshedvorskii, O. Rubinas, V.N. Sorokin, A.N. Smolyaninov, V.V. Vorobyov, A.V. Akimov. *Phys. Rev. Lett.*, **126**, 197702 (2021).
- [13] E. Bernardi, R. Nelz, S. Sonusen, E. Neu. *Crystals*, **7**, 124 (2017).
- [14] I. Stenger, M.-A. Pinault-Thaury, N. Temahuki, R. Gillet, S. Temgoua, H. Bensalah, E. Chikoidze, Y. Dumont, J. Barjon. *J. Appl. Phys.*, **129**, 105701 (2021).
- [15] R. G. Farrer. *Solid State Commun.*, **7**, 685 (1969).
- [16] F.J. Heremans, G.D. Fuchs, C.F. Wang, R. Hanson, D.D. Awschalom. *Appl. Phys. Lett.*, **94**, 152102 (2009).
- [17] A.M. Zaitsev. *Optical properties of diamond: a data handbook* (Springer, Berlin–N. Y., 2001).
- [18] M.N.R. Ashfold, J.P. Goss, B.L. Green, P.W. May, M.E. Newton, C.V. Peaker. *Chem. Rev.*, **120** (12), 5745 (2020).
- [19] T. Tachibana, B.E. Williams, J.T. Glass. *Phys. Rev. B*, **45**, 11975 (1992).
- [20] M. Yokoba, Y. Koide, A. Otsuki, F. Ako, T. Oku, M. Murakami. *J. Appl. Phys.*, **81**, 6815 (1997).
- [21] Y.G. Chen, M. Ogura, S. Yamasaki, H. Okushi. *Semicond. Sci. Technol.*, **20**, 860 (2005).
- [22] T.V. Blank, Yu.A. Goldberg, FTP, **41** (11), 1281 (2007). (in Russian).
- [23] I.J. van der Pauw. *Philips Res. Rep.*, **13**, 1 (1958).
- [24] Y.N. Palyanov, I.N. Kupriyanov, A.F. Khokhryakov, V.G. Ralchenko. *Cryst. Growth of Diamond*, Chap. 17 in *Handbook of Crystal Growth*, ed. by P. Rudolph (Elsevier B.V., 2015).
- [25] Y.N. Palyanov, Y.M. Borzdov, A.F. Khokhryakov, I.N. Kupriyanov. *A.G. Sokol. Cryst. Growth Des.*, **10**, 3169 (2010).
- [26] *Novel Aspects of Diamond. From Growth to Applications*, ed. by Nianjun Yang (Heidelberg, Springer Verlag GmbH, Germany, 2015).
- [27] I.J.R. Chwang, B.J. Smith, C.R. Crowell. *Solid State Electron.*, **17**, 1217, (1974).

Translated by Y.Alekseev